

Xu, Q., Chen, T., Hu, Y. & Gong, P. (2014). Write Pattern Format Algorithm for Reliable NAND-Based SSDs. IEEE Transactions on Circuits and Systems II: Express Briefs, 61(7), pp. 516-520.  
doi: 10.1109/TCSII.2014.2327332



**CITY UNIVERSITY  
LONDON**

[City Research Online](#)

**Original citation:** Xu, Q., Chen, T., Hu, Y. & Gong, P. (2014). Write Pattern Format Algorithm for Reliable NAND-Based SSDs. IEEE Transactions on Circuits and Systems II: Express Briefs, 61(7), pp. 516-520. doi: 10.1109/TCSII.2014.2327332

**Permanent City Research Online URL:** <http://openaccess.city.ac.uk/8194/>

### Copyright & reuse

City University London has developed City Research Online so that its users may access the research outputs of City University London's staff. Copyright © and Moral Rights for this paper are retained by the individual author(s) and/ or other copyright holders. All material in City Research Online is checked for eligibility for copyright before being made available in the live archive. URLs from City Research Online may be freely distributed and linked to from other web pages.

### Versions of research

The version in City Research Online may differ from the final published version. Users are advised to check the Permanent City Research Online URL above for the status of the paper.

### Enquiries

If you have any enquiries about any aspect of City Research Online, or if you wish to make contact with the author(s) of this paper, please email the team at [publications@city.ac.uk](mailto:publications@city.ac.uk).

# Write Pattern Format Algorithm (WPFA) for Reliable NAND-based SSDs

Quan Xu, Thomas M. Chen, *Senior Member, IEEE*, Yu-peng Hu, and Pu Gong

**Abstract**—This paper presents and evaluates a pre-coding algorithm to reduce power consumption and improve data retention in NAND-based solid-state drives (SSD). Compared to the state-of-the-art asymmetric coding and stripe elimination algorithm (SPEA), the proposed write pattern format algorithm (WPFA) achieves better data retention while consuming less power. The hardware for WPFA is simpler and requires less circuitry. The performance of WPFA is evaluated by both computer simulations and FPGA implementation.

**Index Terms**—Solid-state drive, reliability, NAND flash memory, power consumption.

## I. INTRODUCTION

NAND flash memory is the most popular storage technology for solid-state drives due to its non-volatility, lightweight package, and low-power consumption. Basically, each NAND flash cell consists of a floating gate transistor whose threshold voltage can be programmed by injecting certain amounts of charge into the floating gate [?]. For multi-level cell (MLC) NAND flash, one memory cell generally stores more than one bit belonging to different pages that are sequentially programmed at different times. Considering two-bit/cell MLC as an example, the cell threshold voltages, denoted by  $V_{th}$ , are divided into four adjacent levels ( $L0 \leftrightarrow 11$ ,  $L1 \leftrightarrow 01$ ,  $L2 \leftrightarrow 00$ ,  $L3 \leftrightarrow 10$ ) after the sequential programming.

Loss or gain of charge occurring on the floating gate over time will lead to bit flipping and consequently retention failures. Experimental measurements have suggested that bit flipping errors are not random but asymmetric; specifically, only “0 → 1” errors occur in the lower pages and “1 → 0” errors are dominant in the upper pages [?]. Hence, in order to reduce the retention error rate, it is useful to distribute more 1’s to lower pages while more 0’s to upper pages, in other words, program most of the cells to states “11” and “01” and fewer cells to “10”.

Besides retention reliability, another practical problem is the increasing power required for scaling to larger bit-line capacitances. In SSDs, more power is being consumed to charge or discharge the parasitic capacitance of the bit-lines (BLs). The average current consumed during programming is given by

$$I_{pre} = C_{bl} \frac{\Delta V}{T_{pre}} n_{bl} \quad (1)$$

Quan Xu, Thomas M Chen, and Pu Gong are with the School of Engineering and Mathematical Sciences, City University London, EC1V 0HB, U.K. (e-mail: {Quan.Xu.1, Tom.Chen.1, Pu.Gong.1}@city.ac.uk)

Yu-peng Hu is with the Hu Nan University, Changsha 410082, P.R. China. (e-mail: yphu@hnu.edu.cn)

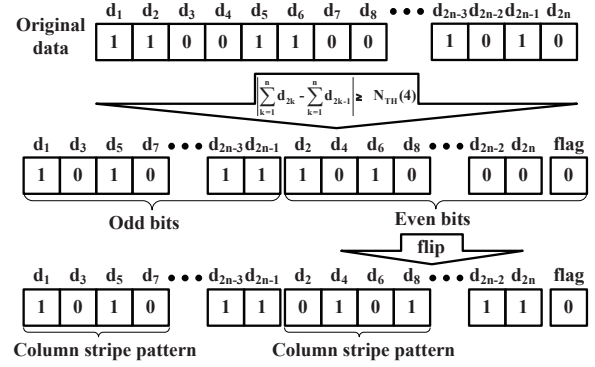


Fig. 1: Example of SPEA

where  $n_{bl}$  the number of bit-lines charged in parallel;  $\Delta V$  is the change of bit-line voltage applied in a program operation;  $C_{bl}$  is the capacitance; and  $T_{pre}$  is pre-charging time [?]. If the programming data contains too many column stripe patterns (CSPs), these bit-line capacitances will be charged and discharged frequently during the programming, increasing the current flow (and SSD power consumption) and possibly leading to malfunctions [?].

Several approaches have been proposed to address the problems of data retention and power [? ? ? ?]. Among these, asymmetric coding and the stripe pattern elimination algorithm (SPEA) proposed by Tanakamaru et al. [?] have been shown to perform well by processing data patterns. In the first step, asymmetric coding calculates the number of 1’s in the input data which is then used to determine whether the bits within the unit are flipped or not. As a result, the distribution of 1’s becomes asymmetric, and the number of cells at high  $V_{th}$  decreases. Secondly, SPEA calculates the difference between the numbers of 1’s in even and odd columns of the original data. If the difference is higher than a threshold value, bits will be rearranged to eliminate the CSPs, which relieves the power problem.

Even though asymmetric coding and SPEA improve SSD performance considerably, their implementation is fairly complex especially when the code length of SPEA increases. Meanwhile, additional CSPs are introduced during the SPEA processing which could cause power problems as well. Consider the example shown in Fig. 1 where the threshold value, denoted as  $N_{TH}$ , is set to 4, and SPEA is applied since the calculated difference is higher than  $N_{TH}$ . After rearranging, long CSPs can be observed in both even and odd bits of the modified data. In this paper, our goal is an efficient solution

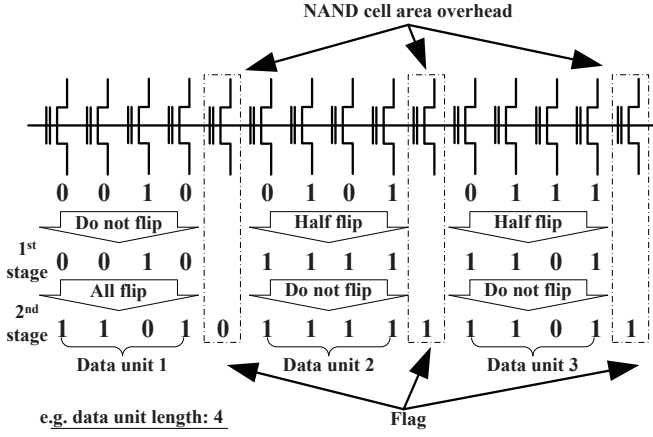


Fig. 2: Proposed WPGA

to the problems above with low complexity implementation. We first present a write pattern format algorithm (WPGA) that carries out asymmetric processing and stripe elimination simultaneously, which allows data patterns to be modified only once before being fed to an error correction coding (ECC) module. Here it should be noted that the advantages of the solution comes at the cost of a small loss of performance compared to asymmetric coding. WPGA will achieve an improvement over the original SPEA approach by avoiding the extra CSPs introduced in SPEA and reducing power consumption. The hardware circuitry for WPGA is shown to use fewer gates and registers, and improve system complexity and latency. Simulation and implementation results show a considerable reduction of both NAND cell overhead and FPGA resource utilization. The trade-offs between complexity and performance are analyzed quantitatively.

## II. WRITE PATTERN FORMAT ALGORITHM

Fig. 2 illustrates an example of the proposed WPGA with lower page input data. The presented solution has two primary stages. The first stage modifies the program data to eliminate the column stripe patterns; the second stage increases the number of 1's. Note that the length of data processing unit has been restricted to  $2^n$  with  $n = 2, 3, 4, 5, \dots$  (although  $n = 2$  is not practical). Initially, all bits of the data unit are added together and the result is stored in an  $n$ -bit sum register. For example, in Fig. 2, the length of data unit is 4 bits and the width of the sum register is 2 bits. The flag in the figure is the most significant bit (MSB) of the sum register which indicates whether the majority of bits in the data unit are 0 or 1. WPGA eliminates CSPs in the following way. If the flag equals 0, the data unit is passed unmodified to the next processing stage, such as "data unit 1" in Fig. 2. If the flag equals 1, a column stripe sequence is added to the input data, and the modulo-2 result is taken as "first stage data", in other words, half of the input data will be flipped. In the example shown in Fig. 2, both "data unit 2" and "data unit 3" are half-flipped. As a result of the first stage, a column stripe pattern (data unit 2) has been eliminated.

To demonstrate the impossibility of extra CSPs, consider two specific data patterns: all-zeros and all-ones as shown in

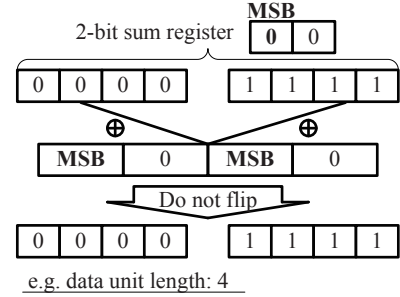


Fig. 3: Analysis of two specific data patterns

Fig. 3. Only these two types of patterns are possible to cause extra CSPs if half-flipping operations are performed. Half-flipping will not be performed for these two types of input since the flag will be 0 in both cases (in the case of the all-ones data pattern, the MSB of the sum register will be 0 due to overflow). Without half flipping, these two types of input will not create extra CSPs.

Concerning data retention, the worst case occurs if all of the memory cells are programmed to the highest  $V_{th}$  level. To avoid that, randomized interleaving may be used, in which the probability of "10" and "00" is about 25% of the total data on the condition that the output data is completely random. In WPGA, retention reliability has been further improved by increasing "1"- and "0"-data of lower and upper pages, respectively. At the second stage, the flag (MSB of the sum register) continues to be used for determining whether the "first stage data" is flipped or not. If the flag equals 0, indicating that the majority in the input data pattern are zeros, all bits of the "first stage data" are flipped, such as the example of "data unit 1" in Fig. 2. On the other hand, if the flag equals 1, the "first stage data" will not be modified, as shown in the examples of "data unit 2" and "data unit 3". Consequently, the number of 1's in lower pages data increases. This part of WPGA is similar to asymmetric coding; however, in the corresponding circuit, as discussed in Section IV, the comparator and multiplexer have been replaced with only XOR gates, thus resulting in simpler circuitry. At the end of the algorithm, "second stage data" together with flag bits are used to form the output. For the data patterns processing of upper pages, the idea is the same except the goal is to decrease the number of 1's.

## III. PERFORMANCE EVALUATION

This section presents simulation results of WPGA for comparison with randomized interleaving and Tanakamaru's asymmetric and SPEA approaches. In these simulations, the data unit length of WPGA is set to be the same as asymmetric coding for fair comparisons.

### A. Maximum Length of Column Stripe Patterns

A figure of merit for energy savings is taken to be the maximum length of column stripe patterns after processing. Let  $M$  and  $N$  denote the code lengths of WPGA and SPEA, respectively. According to Fig. 2, the maximum length of CSPs for the proposed WPGA is  $M - 1$ , whereas that of SPEA

is  $N/2 - N_{TH}$  (based on Fig. 1). Since  $N \gg M$  [? ], the maximum length of CSPs has been substantially reduced which suggests the memory system is better protected from potential damage by current spikes.

### B. Average Program Current

Apart from the maximum length of stripe patterns, the average program current is another performance metric for energy saving. The bit-line capacitance of a NAND flash memory is composed of the inter bit-line capacitance  $C_{bl-bl}$  and other capacitances  $C_{others}$  [? ]. In case that the program data of the memory cell connected to the  $n_{th}$  bit-line  $BL_n$  is 1,  $BL_n$  will be pre-charged to  $V_{cc}$ , and therefore the program data of memory cells connected to  $BL_{n-1}$  and  $BL_{n+1}$  determine whether the inter bit-line capacitance is charged or not. If both adjacent bit-lines,  $BL_{n-1}$  and  $BL_{n+1}$  are pre-charged to  $V_{cc}$ ,  $BL_n$  will only charge  $C_{others}$  because the effect of  $C_{bl-bl}$  will have been eliminated. If both adjacent bit-lines are not pre-charged,  $BL_n$  will charge  $C_{others}$  and two  $C_{bl-bl}$  because  $BL_{n-1}$  and  $BL_{n+1}$  are biased to  $V_{ss}$  (column stripe pattern). In the last possible case, one of the adjacent bit-lines is pre-charged to  $V_{cc}$ , in which case  $BL_n$  charges  $C_{others}$  and one  $C_{bl-bl}$ .

Considering these three cases and assuming that charging the bit-lines is the dominant component of the program current, we can then calculate the average current per page-programming according to Eq. (1). To this end, we built a simulator based on 2 bits/cell MLC having the page length of 8 KB and 256 pages per block. The simulator uses the physical parameters of NAND flash memory presented by Fukuda et al. [? ] where  $C_{bl-bl}$  and  $C_{others}$  occupy 78% and 22% of the total bit-line capacitance, respectively. We assume  $1 \mu s$  charging time and consider three memory systems with random data input. SPEA and asymmetric coding are employed in the first system while WPGA is employed in the second one. The third system is used as a reference since it does not use power saving scheme and employs asymmetric coding only.

The average page-programming current is calculated when 16 blocks data are written to the memory systems. The reduced program current over the reference system as the bit-line capacitance increases is shown in Fig. 4. In this experiment, the data unit length is set to 8 and  $N_{TH}$  of SPEA is set to 6. It has been observed that in terms of energy consumption, the system employed with WPGA outperforms the system employed with SPEA whose codeword is larger than 257 bits. Since the large codeword is generally used in SPEA to reduce flag overhead, WPGA will typically be advantageous.

### C. Proportion of the Highest $V_{th}$ State

To theoretically analyze the proportion of NAND cells on the highest  $V_{th}$  state, it is necessary to derive the amount of 1's in lower pages (or 0's in upper pages) of programming data, which is calculated in the following way.

All possible input patterns are divided into two groups: A and B, by the MSB of the sum register, as shown in Fig. 5. For group A with MSB=0, the second stage of the algorithm

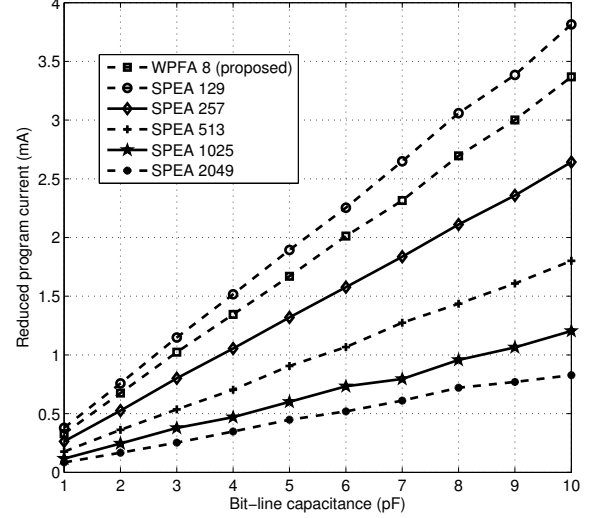


Fig. 4: Reduced program current over the system without power saving scheme

User data length: 2N bits				
	k: Number of "1" s	Number of patterns	Number of "1" s after precoding	Flag
Group A: All flip	0	$C_{2N}^0$	2N-0	"0"
	1	$C_{2N}^1$	2N-1	"0"
	⋮	⋮	⋮	⋮
	N-1	$C_{2N}^{N-1}$	2N-(N-1)	"0"
	2N	$C_{2N}^{2N}$	2N-2N	"0"
Group B: Half flip	N	$C_{2N}^N$		"1"
	N+1	$C_{2N}^{N+1}$		"1"
	⋮	⋮		⋮
	2N-1	$C_{2N}^{2N-1}$		"1"

Fig. 5: Data patterns before and after WPGA processing

is performed and the number of 1's (with flag bits) is given by

$$N_1^A = \sum_{k=0}^{N-1} C_{2N}^k (2N - k) \quad (2)$$

where  $C_n^k$  is the binomial coefficient  $C_n^k = \frac{n!}{k!(n-k)!}$ . For group B with MSB=1, the first stage of the algorithm is performed and only half of the bits are flipped. It is not possible to exactly determine the number of 1's for each individual data pattern, which is the reason it is not shown in Fig. 5. Nonetheless, the total number of 1's after processing can still be calculated taking advantage of symmetry. If we think of the number of 1's related to flags, the total number of 1's in group B after WPGA processing is expressed as

$$N_1^B = \sum_{k=N}^{2N-1} C_{2N}^k (2N) - \frac{1}{2} \sum_{k=N}^{2N-1} C_{2N}^k (k) + \sum_{k=N}^{2N-1} C_{2N}^k \quad (3)$$

Since the total number of data patterns is  $2^{2N} \times (2N + 1)$ , the probability of 1's ( $P_1$ ) is calculated by dividing the number

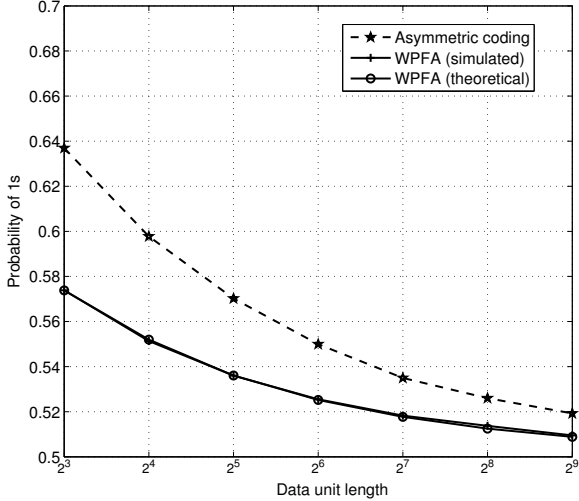


Fig. 6: Simulation results of probabilities of “1”s in Tanakamaru’s and the proposed schemes

of 1’s in all data patterns with flag bits by  $2^{2N} \times (2N + 1)$ , which is

$$P_1 = \frac{N_1^A + N_1^B}{2^{2N} \times (2N + 1)} = \frac{\sum_{k=N}^{2N-1} C_{2N}^k (N + 1) + \sum_{k=0}^{N-1} C_{2N}^k (2N - k)}{2^{2N} \times (2N + 1)} \quad (4)$$

Note that for the flag bits, we could choose either 1 or 0 for the specific group; however, setting the flag bits of group B to be 1 can increase the probability of 1’s of the output bit stream, and the condition is adverse for the upper pages.

In computer simulations, we measured the probability of 1’s of lower pages data for both asymmetric and WPGA encoder, as illustrated in Fig. 6. When the length of input data is large enough, the simulated probability of 1’s for WPGA is fairly close to its theoretical counterpart. Performance loss has been observed in the proposed design comparing to asymmetric coding because of the half-flip operations. At the unit length of  $2^4$ , this loss is about 5% in the target of 1’s probability. However, the performance gap between these two schemes gets smaller when the data unit length increases. In the design of SSD systems, if we set the data unit length to be  $2^4$ , the WPGA will modify the data programmed to NAND so that at least 55% of the lower and upper pages are 1’s and 0’s, respectively. As a result, the highest  $V_{th}$  state, “10” occupies 20% of the total data, which has been reduced by 20% compared to randomized interleaving.

#### D. Overhead of NAND Cell Area

Due to the fact that extra flag bits have to be used for SPEA while the proposed scheme shares only one flag bit for both realizations, Tanakamaru’s design consumes more NAND cell area. Fig. 7 depicts the reduced overhead of the system employed with WPGA compared to three systems employed

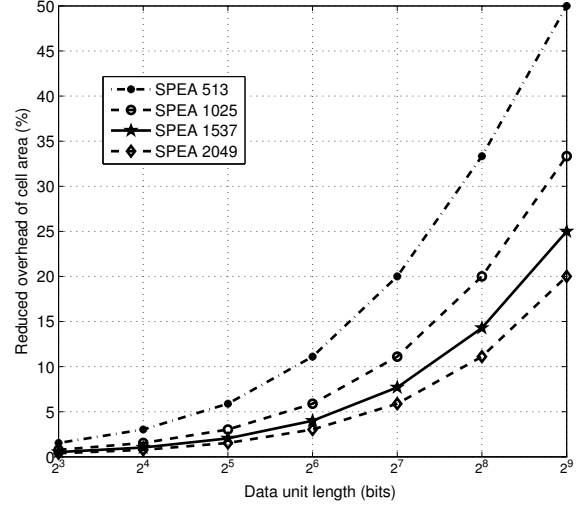


Fig. 7: The reduced NAND cell area overhead to Tanakamaru’s design

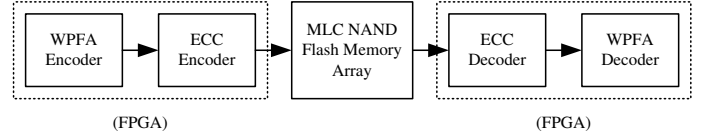


Fig. 8: Framework of coding mechanism in SSDs

with same asymmetric coding and different length of SPEA codeword. It is seen that the reduced overhead increases with data unit length and Tanakamaru’s design consumes even more cell area when the codeword of SPEA gets shorter. For 256-bit data unit and 1025-bit SPEA codeword, the extra cell area of Tanakamaru’s design has been reduced as much as 20%.

#### IV. HARDWARE DESIGN AND IMPLEMENTATION COMPLEXITY

In this section, we consider the logic circuits for the proposed algorithm and propose several ways to reduce the hardware complexity. Generally, WPGA will be implemented together with the ECC module as part of the flash controller in FPGA. The overall framework of FPGA-based flash controller is shown in Fig. 8. Fig. 9 illustrates the circuit structure for the WPGA of 16-bit data unit. Before write patterns processing, the parallel 16-bit data and upper/lower-page select signal (U/L) are generated from information bit stream by the serial/parallel converter. The number of 1’s in the data unit is then calculated with 16-bit adder circuit and the MSB of the 4-bit sum register is used as the judge signal for the subsequent computations. In the proposed circuit, comparators and multiplexers have been replaced with simple XOR gates to perform bit-flipping operations. The flag bit is created through a series of logic operations over MSB and U/L. For Tanakamaru’s design, upper page and lower page asymmetric encoders are implemented with a separate circuit unit. These two encoders for WPGA are integrated in a single circuit which saves FPGA resources. Note that the U/L signal will

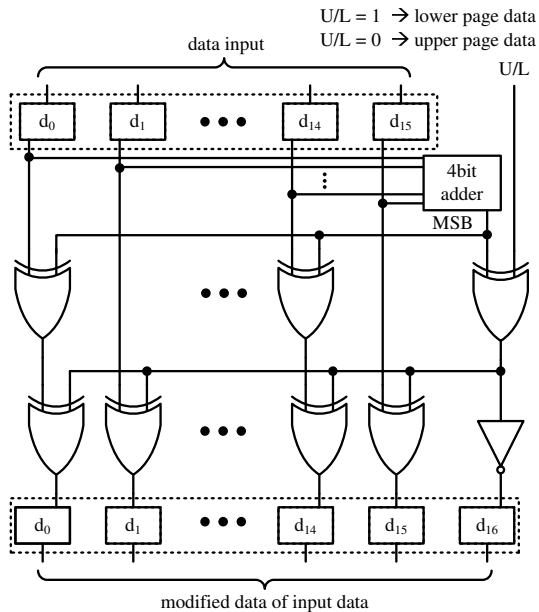


Fig. 9: Circuit schematic of the joint lower/upper pages coding

TABLE I: Comparisons of FPGA Resource Utilization

Encoding Units	ALUTs	Registers	Packed ALMs
Asymmetric (len = 16)	81	34	43
SPEA (len = 129, $N_{TH} = 6$ )	357	150	183
SPEA (len = 257, $N_{TH} = 6$ )	717	281	364
SPEA (len = 513, $N_{TH} = 6$ )	1432	540	727
SPEA (len = 1025, $N_{TH} = 6$ )	2828	1055	1433
WPFA (len = 16)	38	17	19

be correspondingly produced when the flash controller fetches data from the memory array. Hence, in the decoding side, the decoder circuit is easy to implement by performing XOR operations over the input data, the flags and the U/L signal. Due to the fully combinational circuits, the latency, circuit area, and logic resources related to WPFA are small. To quantitatively depict the complexity of each computation unit, we used Verilog to model the proposed circuits. The encoding units were synthesized with Synplify Pro and Altera EP2S180 FPGA according to area optimization. The adaptive look-up tables (ALUTs) and logic registers utilized for each encoding unit are listed in Table I. Results for Tanakamaru's design are included for comparison. In this experiment, the same serial/parallel conversion circuits were assumed for either design thus we only need to compare the complexity of the computation units. As seen, WPFA requires much less logic resources than that of asymmetric coding and SPEA, especially when the code length of SPEA increases. Even compared to the design employed with asymmetric coding only, WPFA still shows lower complexity. The estimated adaptive logic modules (ALMs) used for WPFA encoder is about 8% of the ALMs consumed by Tanakamaru's design for code length of 129 and  $N_{TH}$  of 6 for SPEA. The resource utilization of Tanakamaru's design should be double if considering both lower and upper pages whereas that of the proposed design stays the same.

## V. CONCLUSIONS

In this paper, we present a write pattern formatting algorithm of low complexity to improve the data retention reliability and power consumption of NAND flash based SSDs. The proposed algorithm improves on the existing SPEA approach to completely eliminate column stripe patterns. Furthermore, simulation results show that the overhead for the proposed algorithm is about 80% compared to SPEA using the same parameters. Finally, hardware synthesized results over Altera EP2S180 demonstrate that the implementation complexity of the proposed scheme is much less than that of asymmetric coding and SPEA.

## REFERENCES

- [1] G. Dong, S. Li, and T. Zhang, "Using Data Postcompensation and Predistortion to Tolerate Cell-to-Cell Interference in MLC nand Flash Memory," *IEEE Trans. Circuits Syst. I, Reg. Papers*, vol. 57, no. 10, pp. 2718–2728, Oct 2010.
- [2] S. Tanakamaru, C. Hung, A. Esumi, M. Ito, K. Li, and K. Takeuchi, "95%-lower-BER 43%-lower-power Intelligent Solid-State Drive (SSD) with Asymmetric Coding and Stripe Pattern Elimination Algorithm," in *IEEE Int. Solid-State Circuits Conf. (ISSCC)*, Feb 2011, pp. 204–206.
- [3] R. Micheloni, L. Crippa, and A. Marelli, "Inside NAND Flash Memories," *Springer Press*, Aug 2010.
- [4] S. Tanakamaru, C. Hung, and K. Takeuchi, "Highly Reliable and Low Power SSD Using Asymmetric Coding and Stripe Bitline-Pattern Elimination Programming," *IEEE J. Solid-State Circuits*, vol. 47, no. 1, pp. 85–96, Jan 2012.
- [5] Y.-P. Hu, N. Xiao, and X.-F. Liu, "An elastic error correction code technique for NAND flash-based consumer electronic devices," *IEEE Trans. Consum. Electron.*, vol. 59, no. 1, pp. 1–8, Feb 2013.
- [6] K. Takeuchi, "Novel Co-Design of NAND Flash Memory and NAND Flash Controller Circuits for Sub-30 nm Low-Power High-Speed Solid-State Drives (SSD)," *IEEE J. Solid-State Circuits*, vol. 44, no. 4, pp. 1227–1234, 2009.
- [7] K.-D. Suh, B.-H. Suh, and Y.-H. Lim, "A 3.3 V 32 Mb NAND Flash Memory with Incremental Step Pulse Programming Scheme," *IEEE J. Solid-State Circuits*, vol. 30, no. 11, pp. 1149–1156, Nov 1995.
- [8] K. Fukuda, Y. Watanabe, E. Makino, K. Kawakami, J. Sato, T. Takagiwa, N. Kanagawa, H. Shiga, N. Tokiwa, and Y. Shindo, "A 151-mm<sup>2</sup> 64-Gb 2 Bit/Cell NAND Flash Memory in 24-nm CMOS Technology," *IEEE J. Solid-State Circuits*, vol. 47, no. 1, pp. 75–84, 2012.